Linear Stability of TCP/RED and a Scalable Control *

Steven H. Low Fernando Paganini Jiantao Wang John C. Doyle †

November 22, 2003

Abstract

We demonstrate that the dynamic behavior of queue and average window is determined predominantly by the stability of TCP/RED, not by AIMD probing nor noise traffic. We develop a general multi-link multi-source model for TCP/RED and derive a local stability condition in the case of a single link with heterogeneous sources. We validate our model with simulations and illustrate the stability region of TCP/RED. These results suggest that TCP/RED becomes unstable when delay increases, or more strikingly, when link capacity increases. The analysis illustrates the difficulty of setting RED parameters to stabilize TCP: they can be tuned to improve stability, but only at the cost of large queues even when they are dynamically adjusted. Finally, we present a simple distributed congestion control algorithm that maintains stability for arbitrary network delay, capacity, load and topology.

1 Introduction

It is well known that TCP/RED can oscillate wildly and it is extremely hard to reduce the oscillation by tuning RED parameters, e.g., [14, 4]. The additive-increase-multiplicative-decrease (AIMD) strategy employed by TCP Reno (and its variants such as NewReno and SACK) and noise-like traffic that are not effectively controlled by TCP no doubt contribute to this oscillation. Recent models e.g., [6, 8], imply however that oscillation is an inevitable outcome of the protocol itself. We present more evidence to support this view (Section 2). We argue that TCP/RED oscillates not only because of its AIMD probing, and not only because of noise traffic (e.g., short lived TCP connections), but more fundamentally, it is due to instability[1]. We illustrate using *ns-2* simulations

*Appeared in **Computer Networks Journal, 43(5):633-647, December 2003**

†J. C. Doyle, S. H. Low and J. Wang are with California Institute of Technology; emails: {doyle,jiantao}@cds.caltech.edu, slow@caltech.edu. F. Paganini is with University of California, Los Angeles; email: paganini@ee.ucla.edu. Preliminary version has appeared in [11]. We acknowledge the supports of NSF through grants ANI-0113425 and ANI-0230967 and AFOSR through grant F49620-03-1-0119.

[1]By this, we mean that even if window is not adjusted on each acknowledgment arrival or loss event, but is adjusted periodically by the same *average* amount AIMD would over the same period, the oscillation persists.

that, after smoothing out the AIMD component of the oscillation, the average behavior can either be steady with small random fluctuations (when the protocol is stable), or exhibit limit cycles of amplitude much larger than random fluctuations (when it is unstable). Moreover, this qualitative behavior persists even when a large amount of noise traffic is introduced, and even when sources have different delays. We conclude that it is stability that largely determines the dynamics of TCP/RED.

This motivates the stability characterization of TCP/RED. In Section 3 we develop a general nonlinear model of TCP/RED. The equilibrium structure of this model is analyzed in [12] by interpreting various TCP/AQM as carrying out distributed primal-dual algorithms over the Internet to maximize aggregate source utility in the form of congestion control. Here, we study local stability by linearizing the model around the equilibrium. The linear model generalizes the single-link identical-source model of [8]. We validate our model with simulation results and illustrate the stability region of TCP/RED. We derive a sufficient stability condition for the special case of a single link with *heterogeneous* sources. It shows that TCP/RED becomes unstable when delay increases, or more strikingly, when link capacity increases!

The gain introduced by TCP increases rapidly with delay and link capacity. This induces instability and makes compensation by RED extremely difficult. In particular, RED parameters can be tuned to improve stability, but only at the cost of a large queue, even when they are dynamically adjusted.

This suggests that the current protocol is ill-suited for future networks where capacity will be large. In Section 6 we present a simple congestion control algorithm, developed in [15], that can be implemented in a decentralized manner by sources and links, and that maintains linear stability for *arbitrary* delay, capacity, load and routing. Moreover, it achieves high network utilization in equilibrium with negligible queues. It demonstrates that it may be unnecessary to sacrifice stability for performance. Extensions of this algortihm to achieve arbitrary fairness, implementation strategies and simulation results can be found in [16].

2 Why does TCP/RED oscillate?

What is the effect of AIMD, noise traffic, and heterogeneity of delays have on average window and instantaneous queue? In this section, we show that their effect pales in comparison with that of protocol instability.

We simulate in *ns-2* a single bottleneck link with capacity 9 pkts/ms (constant packet size = 1000bytes). The link runs RED with ECN marking in 'byte' mode (i.e., acknowledgment packets are marked with negligible probability). The RED parameters are `max_p` $= 0.1$, `min_th` $= 50$ pkts, `max_th` $= 550$ pkts, and weight for queue averaging $\alpha = 10^{-4}$. The link is shared by 50 persistent FTP sources. We have run simulations with both one-way and two-way traffic, and the behavior is very similar. The results in Figures 1 and 2 are for two-way traffic, and those in Figure 3 are for one-way traffic. Of the measurements from live Internet in [1], 85% have round trip times between

15-500ms. We perform simulations within this range of delays.

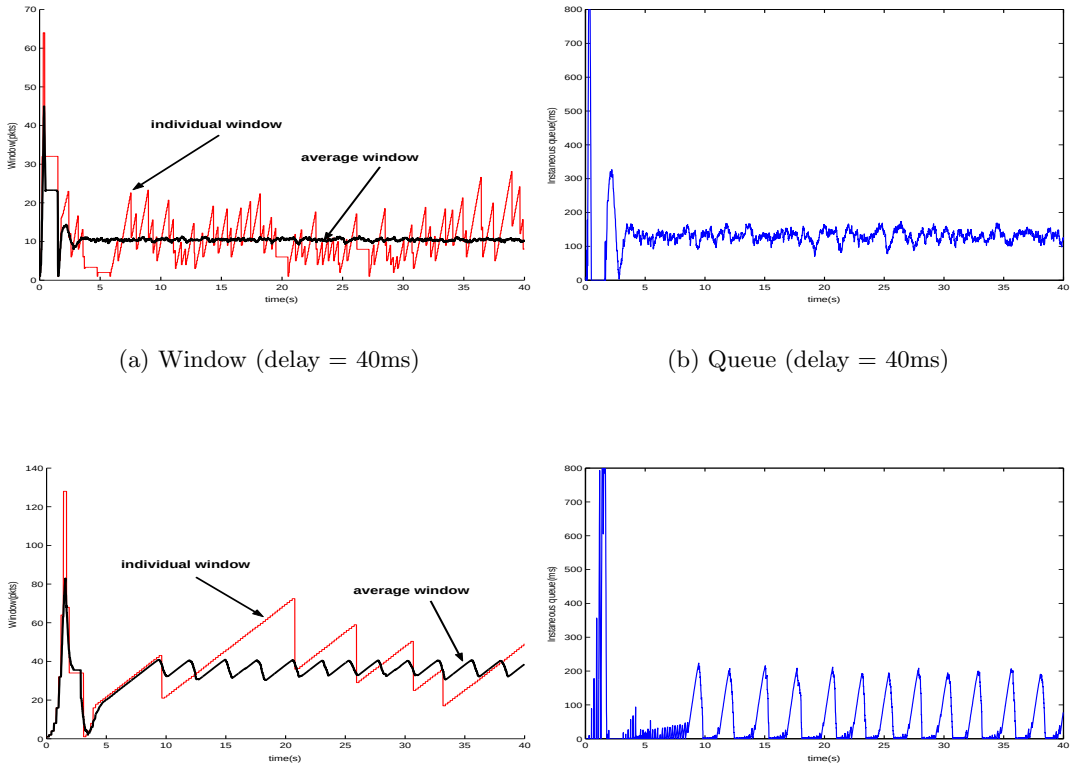

(a) Window (delay = 40ms)

(b) Queue (delay = 40ms)

(c) Window (delay = 200ms)

(d) Queue (delay = 200ms)

Figure 1: Window and queue traces without noise traffic. Simulation parameters: 50 sources, capacity = 9 pkts/ms, RED = (0.1, 50, 550, 10^{-4}), marking with 'byte' mode; two-way traffic.

Figure 1 gives the result of two cases where connections have identical round trip propagation delay and generate traffic in both directions. Figure 1(a) shows an individual window (light curve) and the average window (dark curve), averaged over all 50 sources, both as a function of time. They are typical traces when round trip propagation delay is small (40ms in this case). Oscillations due to Reno's AIMD are prominent in the individual window, but disappear in the average window. As one would expect, since the queue averages individual windows, it also displays a smooth trace with small random fluctuations, as shown in Figure 1(b). We consider the *average* behavior of the protocol stable (non-oscillatory) in this case.

Figures 1(c) and (d) show the corresponding windows and queue when round trip propagation

delay is increased to 200ms. Not only does the individual window oscillate with a larger amplitude, more importantly, its average displays a deterministic limit cycle. This also shows up in the queue trace. We say the protocol is in an *unstable* regime.

What is the effect of noise-like mice traffics that are not effectively controlled by TCP/RED? To get a qualitative understanding, we add short http sources to the 50 persistent bi-directional FTP connections. Each http source sends a single-packet request to its destination, which then replies with a file of size that is exponentially distributed with a mean of 12 1KB-packets. After the source completely receives the data, it waits for a random time that is exponentially distributed with a mean of 500 msec, and repeats the process. Both the request and the response are carried over TCP connections. Two sets of simulations are conducted, the first with 60 http sources generating 10% noise (i.e., persistent FTP sources occupied 90% of bottleneck link capacity), and the second set with 180 http sources generating 30% noise. The queue traces when propagation delay is 40ms (stable) and 200ms (unstable), respectively, are shown in Figures 2(a) and (b) for a noise intensity of 10%, and in Figure 2(c) and (d) for a noise intensity of 30%. The behavior of the queue and average window (not shown here) is dominated by the stability of the protocol, not by noise-like mice traffic (compare with Figures 1(b) and (d)). In the stable regime (40ms delay), the noise traffic increases the average queue length slightly. This increases the marking probability and reduces the average window of the FTP sources.

All our previous simulations are for sources with identical propagation delay. Will the dynamic behavior be very different when sources have different delays? We repeat the previous experiments, without noise, with 50 persistent uni-directional connections having delays ranging from 40ms to 64ms at 1ms increment, with 2 sources to each delay value. We study their dynamic behavior when all delays are scaled up, or down, over a wide range. The behavior is qualitatively similar to the case of identical delay, with more severe queue oscillation. Figure 3(a) shows the instantaneous queue when the scaling factor is 0.3 (delays range from 0.3(40)ms to 0.3(64)ms), with an average delay of 15.6ms, averaged over all sources. Figure 3(b) shows the queue when the scaling factor is 4, with an average delay of 208ms.

Hence it is protocol stability that largely determines the dynamics of TCP/RED. We now characterize when TCP/RED is stable.

3 Dynamic model

In this section we develop a model of TCP/RED and use it to predict the onset of instability. We start with a nonlinear model, make a few remarks about its equilibrium properties, and then linearize the model around the equilibrium. We validate our linear model with *ns-2* simulations, and illustrate the stability region of TCP/RED. Finally we derive a stability condition for the special case of a single link with *heterogeneous* sources.

3.1 Nonlinear model of TCP/RED

A network is modeled as a set of L links (scarce resources) with finite capacities $c = (c_l, l \in L)$. They are shared by a set of N sources indexed by i in set I. Each source i uses a set $L_i \subseteq L$ of links. The sets L_i define an $L \times N$ routing matrix

$$R_{li} = \begin{cases} 1 & \text{if } l \in L_i \\ 0 & \text{otherwise} \end{cases}$$

Associated with each link l is its marking probability[2] $p_l(t)$ at time t, and with each source s its window $w_i(t)$ at time t. TCP Reno prescribes how $w_i(t)$ is adjusted and AQM prescribes how $p_l(t)$ is updated. Together they form a delayed feedback system and can be interpreted as carrying out a distributed primal-dual algorithm to solve a welfare maximization problem over the Internet [12, 13].

Define the round trip time $\tau_i(t)$ of source i at time t by:

$$\tau_i(t) = d_i + \sum_l R_{li} \frac{b_l(t)}{c_l} \tag{1}$$

where d_i is the round trip propagation delay and $b_l(t)$ is the backlog at link l at time t.[3] Define source i's rate $x_i(t)$ at time t as:

$$x_i(t) := \frac{w_i(t)}{\tau_i(t)} \tag{2}$$

The aggregate flow rate at link l is

$$y_l(t) = \sum_i R_{li} x_i(t - \tau_{li}^f(t)) \tag{3}$$

where $\tau_{li}^f(t)$ is the forward delay from source i to link l. The end-to-end marking probability observed at source i is $q_i(t) = 1 - \prod_{l \in L_i}(1 - p_l(t - \tau_{li}^b(t)))$ where $\tau_{li}^b(t)$ is the backward delay from link l to source i. We assume that $p_l(t)$ are small for all t so that, approximately, the end-to-end probability is

$$q_i(t) := \sum_l R_{li} p_l(t - \tau_{li}^b(t)) \tag{4}$$

[2]By 'marking', we mean either dropping a packet or setting an ECN (Explicit Congestion Notification) bit in the packet.

[3]This is generally not the round trip time experienced by a packet, which visits different links in its path at different times and hence experiences queueing delays of various links at different times. This expression however sums the queueing delay of different links at the *same time* t.

a sum of delayed link probabilities. The forward and backward delays are related to the round trip time through:

$$\tau_i(t) \;=\; \tau^f_{li}(t) + \tau^b_{li}(t)$$

for all $l \in L_i$.

We now model TCP Reno and RED. We focus on the AIMD algorithm of TCP Reno (and its variants such as NewReno and SACK). At time t, source i transmits at rate $x_i(t)$ packets/sec; hence, it receives acknowledgments at rate $x_i(t-\tau_i(t))$, assuming every packet is acknowledged. A fraction $(1-q_i(t))$ of these acknowledgments are positive, each incrementing the window $w_i(t)$ by $1/w_i(t)$; hence the window $w_i(t)$ increases, on average, at the rate of $x_i(t-\tau_i(t))(1-q_i(t))/w_i(t)$. Similarly negative acknowledgments are received at an average rate of $x_i(t-\tau_i(t))q_i(t)$, each halving the window, and hence the window $w_i(t)$ decreases at a rate of $x_i(t-\tau_i(t))q_i(t)w_i(t)/2$. Hence, the window evolves under Reno according to

$$\begin{aligned}\dot{w}_i(t) \;&=\; x_i(t-\tau_i(t))(1-q_i(t))\frac{1}{w_i(t)} \\ &\quad - x_i(t-\tau_i(t))q_i(t)\frac{w_i(t)}{2}\end{aligned} \tag{5}$$

where $q_i(t)$ is given by (4).

To model RED, let $b_l(t)$ denote the instantaneous queue length at time t that evolves according to, when $b_l(t) > 0$,

$$\dot{b}_l(t) \;=\; y_l(t) - c_l \tag{6}$$

where $y_l(t)$ is the flow rate given by (3) and c_l is the link capacity. Define the average queue length as $r_l(t)$. It is updated according to:

$$\dot{r}_l(t) \;=\; -\alpha_l c_l\,(r_l(t) - b_l(t)) \tag{7}$$

for some constant $0 < \alpha_l < 1$. Given the average queue length $r_l(t)$, the marking probability is given by

$$p_l(t) \;=\; \begin{cases} 0 & r_l(t) \le \underline{b}_l \\ \rho_l r_l(t) - \rho_l \underline{b}_l & \underline{b}_l < r_l(t) < \overline{b}_l \\ \eta_l r_l(t) - (1 - 2\overline{p}_l) & \overline{b}_l \le r_l(t) < 2\overline{b}_l \\ 1 & r_l(t) \ge 2\overline{b}_l \end{cases} \tag{8}$$

where $\underline{b}_l, \overline{b}_l$, and $\overline{p}_l$ are RED parameters, and

$$\rho_l \;:=\; \frac{\overline{p}_l}{\overline{b}_l - \underline{b}_l} \qquad \text{and} \qquad \eta_l \;:=\; \frac{1-\overline{p}_l}{\overline{b}_l}$$

In summary, TCP/RED is modeled by (5–8) and their interconnection through the network is modeled by (3–4).

Remarks:

1. In [12, 13], we interpret the TCP/RED model (5)–(8) and other TCP/AQM models as carrying out distributed primal-dual algorithms to maximize aggregate source utility over the Internet. We regard source rates $x_i(t)$ as primal variables iterated by TCP, and marking probabilities $p_l(t)$ as dual variables (Lagrange multipliers) iterated by AQM. Different protocols correspond to different update rules and they maximize different utility functions U. The utility function of TCP Reno is derived to be:

$$U_i(x_i) \;=\; \frac{\sqrt{2}}{\tau_i}\,\tan^{-1}\left(\frac{\tau_i x_i}{\sqrt{2}}\right)$$

   whereas that of TCP Vegas [3] is:

$$U_i(x_i) \;=\; \alpha \log x_i$$

   Given any network topology R, link capacities c, and TCP utility U_i, we can determine any equilibrium properties of interest by solving a simple convex program. These include throughput, loss, delay, interaction of different TCP protocols and fairness of their equilibrium rate allocation.

2. Many implementations of Reno, or its variants, halves its window at most once in each round trip time (so does *ns-2*). In this case, the multiplicative decrease term in (5) should be replaced by $-q_i(t)w_i(t)/2\tau_i(t)$. For all simulations in this paper, the marking probability is so small that the probability of having multiple marks in a round trip time is negligible. Hence the difference between the two models of multiplicative decrease is negligible, as confirmed by the validation simulations below.

3.2 Linear model of TCP/RED

We linearize the TCP/RED equations (5-8) to study its stability around equilibrium. We make several simplifying assumptions. First we assume that the routing matrix R has full row rank so there is a unique equilibrium loss probability vector p (Lagrange multiplier). Second we assume that only bottleneck links, whose equilibrium marking probability is strictly positive, are included in the model. Moreover we assume that the system operates in the region $\underline{b}_l < r_l(t) < \overline{b}_l$, so that the marking probability is affine in the average queue length, $p_l(t) = \rho_l(r_l(t) - \underline{b}_l)$. Finally, we make a key assumption on the time-varying round trip delay.

Round trip delay appears in two places: first, in the relation between window $w_i(t)$ and rate $x_i(t)$, as expressed in (2), and second, in the time argument of flow rate $y_l(t)$, as expressed in (3), and

the end-to-end marking probability $q_i(t)$, as expressed in (4). Inclusion of instantaneous queueing delay in the first place yields a qualitatively different model than if queueing delay is ignored or assumed constant. It means that the queue is not an integrator but has a more complicated dynamics; see (11) below. As the proof of Theorem 2 shows, this dynamic is critical to the stability of TCP/RED. The resulting linear model matches simulations significantly better than if queueing delay is assumed constant. Time-varying delay in the second place makes linearization difficult, and we replace it by its (constant) equilibrium value (including equilibrium queueing delay). Hence, we use the time-varying delay (1) in (2), but approximate the delays $\tau_i(t)$, $\tau_{li}^f(t)$, $\tau_{li}^b(t)$ by their equilibrium values in (3) and (4).

With these assumptions, we linearize Reno/RED around the unique equilibrium. From (5), Reno becomes:

$$\begin{aligned}\dot{w}_i(t) &= \left(1-\sum_l R_{li}p_l(t-\tau_{li}^b)\right)\frac{w_i(t-\tau_i)}{\tau_i(t-\tau_i)}\,\frac{1}{w_i(t)} \\ &\quad -\frac{1}{2}\sum_l R_{li}p_l(t-\tau_{li}^b)\,\frac{w_i(t-\tau_i)\,w_i(t)}{\tau_i(t-\tau_i)}\end{aligned}$$

Let $w_i^*, p_l^*, \ldots$ denote equilibrium quantities and $\delta w_i(t) = w_i(t) - w_i^*$, $\delta p_l(t) = p_l(t) - p_l^*, \ldots$. Linearization then yields:

$$\delta\dot{w}_i(t) = -\frac{1}{\tau_i q_i^*}\sum_l R_{li}\delta p_l(t-\tau_{li}^b) - \frac{q_i^* w_i^*}{\tau_i}\delta w_i(t)$$

where $q_i^* = \sum_l R_{li}p_l^*$ is the equilibrium end-to-end probability, and $w_i^* = x_i^*\tau_i$ is the equilibrium window.

Around the equilibrium, the buffer process under RED evolves according to:

$$\begin{aligned}\dot{b}_l(t) &= \sum_l R_{li}\frac{w_i(t-\tau_{li}^f)}{\tau_i(t-\tau_{li}^f)} - c_l \\ &= \sum_l R_{li}\frac{w_i(t-\tau_{li}^f)}{d_i+\sum_k R_{ki}b_k(t-\tau_{li}^f)/c_k} - c_l\end{aligned}$$

Let $\tau_i = d_i + \sum_k R_{ki}b_k^*/c_k$ be the equilibrium round trip time (including queueing delay). Linearizing, we have

$$\delta\dot{b}_l(t) = \sum_i R_{li}\frac{\delta w_i(t-\tau_{li}^f)}{\tau_i} - \sum_k\sum_i R_{li}R_{ki}\,\frac{w_i^*}{\tau_i^2 c_k}\,\delta b_k(t-\tau_{li}^f)$$

The second term above is ignored if we have neglected or assumed constant the queueing delay in round trip time. The double summation sums over all links k that share any source i with link

l. It says that the link dynamics in the network is coupled through shared sources. The term $\frac{w_i^*}{\tau_i c_k}\delta b_k(t-\tau_{li}^f)$ is roughly the backlog at link k due to packets of source i, under FIFO queueing. Hence the backlog $b_l(t)$ at link l decreases at a rate that is proportional to the backlog of this shared source i at another link k. This is because backlog in the path of source i reduces the *rate* at which source i packets arrive at link l, decreasing $b_l(t)$.

Putting everything together, Reno/RED is described by, in Laplace domain,

$$\begin{aligned}
\delta w(s) &= -(sI+D_1)^{-1}D_2R_b^T(s)\delta p(s)\\
\delta p(s) &= (sI+D_3)^{-1}D_4\delta b(s)\\
\delta b(s) &= (sI+R_f(s)D_5R^TD_6)^{-1}R_f(s)D_7\delta w(s)
\end{aligned}$$

where the diagonal matrices are $D_1 = \text{diag}\ \left(\frac{q_i^*w_i^*}{\tau_i}\right)$, $D_2 = \text{diag}\ \left(\frac{1}{\tau_i q_i^*}\right)$, $D_3 = \text{diag}\ (\alpha_l c_l)$, $D_4 = \text{diag}\ (\alpha_l c_l \rho_l)$, $D_5 = \text{diag}\ \left(\frac{w_i^*}{\tau_i^2}\right)$, $D_6 = \text{diag}\ \left(\frac{1}{c_l}\right)$, $D_7 = \text{diag}\ \left(\frac{1}{\tau_i}\right)$, and $R_f(s)$ and $R_b(s)$ are delayed forward and backward routing matrices, defined as:

$$[R_f(s)]_{li} = \begin{cases} e^{-\tau_{li}^f s} & \text{if } l \in L_i \\ 0 & \text{otherwise} \end{cases} \tag{9}$$

$$[R_b(s)]_{li} = \begin{cases} e^{-\tau_{li}^b s} & \text{if } l \in L_i \\ 0 & \text{otherwise} \end{cases} \tag{10}$$

This model generalizes the single-link identical-source model of [8] to multiple links with heterogeneous sources.

3.3 Validation and stability region

We present a series of experiments to validate our linear model when the system is stable or barely unstable, and to illustrate numerically the stability region.

We consider a single link of capacity c pkts/ms shared by N sources with identical round trip propagation delay d ms. For $N = 20, 30, \ldots, 60$ sources, capacity $c = 8, 9, \ldots, 15$ pkts/ms, and propagation delay $d = 50, 55, \ldots, 100$ ms, we examine the Nyquist plot of the loop gain of the feedback system ($L(j\omega)$ in (11) below). For each (N, c) pair, we determine the delay $d_m(N, c)$, at 5ms increment, at which the smallest intercept of the Nyquist plot with the real axis is closest to -1. This is the delay at which the system (N, c) transits from stability to instability according to the linear model. For this delay, we compute the critical frequency $f_m(N, c)$ at which the phase of $L(j\omega)$ is $-\pi$. Note that the computation of $L(j\omega)$ requires equilibrium round trip time τ, the sum of propagation delay $d_m(N, c)$ and equilibrium queueing delay. The queueing delay is calculated from the duality model [12]. Hence, for each (N, c) pair that becomes barely unstable at a delay between 50ms and 100ms, we obtain the critical (propagation) delay $d_m(N, c)$ and the critical

frequency $f_m(N,c)$ from the analytical model. For all experiments, we have fixed the parameters at $\alpha = 10^{-4}$, $\rho = 0.1/(540-40) = 0.0002$, and $\beta = 0.5$.

We repeat these experiments in *ns-2*, using persistent FTP sources and RED with ECN marking. The RED parameters are (0.1, 40pkts, 540pkts, 10^{-4}), corresponding to the α and ρ values in the model. For each (N,c) pair, we examine the queue and window trajectories to determine the critical delay $d_{ns}(N,c)$ when the system transits from stability to instability. We measure the critical frequency $f_{ns}(N,c)$, the fundamental frequency of queue oscillation, from the FFT of the queue trajectory. Thus, corresponding to the linear model, we obtain the critical delay $d_{ns}(N,c)$ and frequency $f_{ns}(N,c)$ from simulations.

We compare model prediction with simulation. Figure 4(a) plots the critical delay $d_{ns}(N,c)$ from *ns-2* simulations versus the critical delay $d_m(N,c)$ computed from the linear model. Each data point corresponds to a particular (N,c) pair. The dashed line is where all points should lie if the linear model agrees perfectly with the simulation. Figure 4(b) gives the corresponding plot for critical frequencies $f_{ns}(N,c)$ versus $f_m(N,c)$. The agreement between model and simulation seems quite reasonable (recall that delay values have a resolution of 5ms).

Consider a static link model where marking probability is a function of link flow rate:

$$p_l(t) \quad = \quad f_l(y_l(t))$$

Then the linearized model is

$$\delta p_l(t) \quad = \quad f_l'(y_l^*)\ \delta y_l(t)$$

where $f_l'(y_l^*)$ is the derivative of f_l evaluated at equilibrium. Also shown in Figure 4(b) are critical frequency predicted from this static-link model (with $f_l'(y_l^*) = \rho = 0.0002$; this does not affect the critical frequency), using the same Nyquist plot method described above. It shows that queue dynamics is significant at the time-scale of interest.

Figure 5 illustrates the stability region implied by the linear model. For each N, it plots the critical delay $d_m(N,c)$ versus capacity c. The curve separates stable (below) from unstable regions (above). The negative slope shows that TCP/RED becomes unstable when delay or capacity is large. As N increases, the stability region expands, i.e., small load induces instability. Intuitively, a larger delay or capacity, or a smaller load, leads to a larger equilibrium window; this confirms the folklore that TCP behaves poorly at large window size.

4 Linear stability: single-link heterogeneous sources

We now characterize the stability region in the case of a single link with N *heterogeneous* sources. Writing forward delay as a fraction $\beta_i \in (0,1)$ of round trip time, $\tau_i^f = \beta_i \tau_i$, and dropping link subscript l, the loop gain is

$$L(s) \quad = \quad R_f(s) D_7 (sI + D_1)^{-1} D_2 R_b^T(s) (sI + D_3)^{-1} D_4 (sI + R_f(s) D_5 R^T D_6)^{-1}$$

$$= \sum_i \frac{1}{\tau_i p^*(\tau_i s + p^* w_i^*)} \cdot \frac{\alpha c \rho}{s + \alpha c} \cdot \frac{1}{s + \frac{1}{c}\sum_n \frac{x_n^*}{\tau_n} e^{-\beta_i \tau_n s}} \cdot e^{-\tau_i s} \tag{11}$$

The first term on the right-hand side describes TCP dynamics, the second term RED averaging, the third term buffer process, and the last term network delay. The special case where all sources have identical round trip times, $\tau_i = \tau$, and forward delays are zero, $\beta_i = 0$, is analyzed in [8]. They provide sufficient conditions for closed-loop stability and use them to tune RED parameters α and ρ.

We start with a lemma that collects some equilibrium properties we use below. It can be proved directly from the fixed point of (5)–(8); or see [12]. Let $\overline{\tau} := \max_i \tau_i$, $\underline{\tau} := \min_i \tau_i$, $\hat{\tau} := \left(\sum_i \frac{1}{\tau_i}\right)^{-1}$, and $\overline{\beta} := \max_i \beta_i$. Recall the RED parameters: α is weight in queue averaging and ρ is the slope of marking probability.

Lemma 1 *Let p^* be the equilibrium loss probability, w_i^* and x_i^* be the equilibrium window and rate respectively. Then $p^* = 2/(2 + (c\hat{\tau})^2)$, $w_i^* = c\hat{\tau}$ for all sources i, $x_i^* = w_i^*/\tau_i$ and $\sum_i x_i^*/c = 1$.*

Let

$$\overline{\theta} \;:=\; \pi - \arctan \frac{\pi(1-\overline{\beta})}{2\overline{\beta}} \;\in\; \left(\frac{\pi}{2}, \pi\right) \tag{12}$$

Theorem 2 *The closed-loop system described by (11) is stable if*

$$\rho \frac{\overline{\tau}^2}{\hat{\tau}\underline{\tau} p^{*2} w_1^*} \left(1 + \frac{1}{c\underline{\tau}\alpha} + \frac{1}{p^* w_1^*}\right) \;<\; \frac{\pi(1-\overline{\beta})^2}{\sqrt{4\overline{\beta}^2 + \pi^2(1-\overline{\beta})^2}}$$

Proof. The closed-loop system is stable if $L(s)$ does not pass through $(-1, 0)$ in the complex plane as $s = j\omega$ traverses the Nyquist contour for $\omega = 0$ to ∞. the right-half plane. To show this, re-write (11) as

$$L(s) \;=\; \frac{c^2 \alpha \rho}{p^*} \sum_i \frac{w_i^*/\tau_i}{c} \frac{z_i(s)}{w_i^*}$$

where

$$z_i(s) \;=\; \frac{e^{-\tau_i s}}{(s + \alpha c)(\tau_i s + p^* w_i^*)} \cdot \frac{1}{(s + \sum_n \frac{x_n^*}{c\tau_n} e^{-\beta_n \tau_n s})} \tag{13}$$

Lemma 1 implies that (since w_i^* are equal for all i)

$$L(j\omega) \;=\; \frac{c\alpha\rho}{\hat{\tau}p^*}\;\sum_i \frac{x_i^*}{c}\, z_i(j\omega) \tag{14}$$

i.e., $L(j\omega)$ lies in the convex hull defined by the N points $z_i(j\omega)$ in the complex plane. We will prove that this convex hull is bounded away from $(-1, 0)$, through Lemmas 3–5 whose proofs are relegated to the Appendix.

Lemma 3 *For all $\omega \geq 0$,*

$$L(j\omega) \;\in\; \frac{c\overline{\tau}^2\alpha\rho}{\hat{\tau}p^*(1-\overline{\beta})} \cdot co\left\{r(\omega)e^{-j\phi(\omega)} \cdot e^{-j\theta} \;:\; 0 \leq \theta \leq \overline{\theta},\; \omega \geq 0\right\}$$

where coA is the convex hull of set A, $\overline{\theta}$ is defined in (12), and

$$r(\omega)e^{-j\phi(\omega)} \;:=\; \frac{e^{-j\omega}}{\omega(j\omega + \alpha c_{\underline{\tau}})(j\omega + p^*w_1^*)}$$

Since $r(\omega)$ is decreasing in ω, we can ignore ω for which $\phi(\omega) + \theta < \overline{\theta}$, because the points in the left-half plane where the set in Lemma 3 crosses the real axis are contained in the set

$$A_1 \;:=\; \frac{c\overline{\tau}^2\alpha\rho}{\hat{\tau}p^*(1-\overline{\beta})} \cdot \mathrm{co}\left\{r(\omega)e^{-j\phi(\omega)} \cdot e^{-j\theta} \;:\; 0 \leq \theta \leq \overline{\theta},\; \phi(\omega) + \theta \geq \overline{\theta}\right\}$$

The next lemma says that we can further simplify this set by focusing on just the Nyquist trajectory for $\theta = \overline{\theta}$.

Lemma 4

$$A_1 \;\subseteq\; \frac{c\overline{\tau}^2\alpha\rho}{\hat{\tau}p^*(1-\overline{\beta})} \cdot co\left\{r(\omega)e^{-j\phi(\omega)} \cdot e^{-j\overline{\theta}} \;:\; \omega \geq 0\right\} \;=:\; A_2$$

The next lemma bounds the set A_2 in a half plane.

Lemma 5

$$A_2 \;\subseteq\; \frac{c\overline{\tau}^2\alpha\rho}{\hat{\tau}p^*(1-\overline{\beta})} \cdot \left\{\eta\; e^{-j\overline{\theta}} \;:\; Im\{\eta\} \geq -\lambda\right\}$$

where

$$\lambda \;:=\; \frac{1}{\alpha c_{\underline{\tau}} p^* w_1^*}\left(1 + \frac{1}{\alpha c_{\underline{\tau}}} + \frac{1}{p^*w_1^*}\right) \tag{15}$$

The half plane in Lemma 5 is shown in Figure 6. From the figure, the set, and hence $L(j\omega)$, is to the left of $(-1, 0)$ if

$$1 \quad > \quad \frac{c\overline{\tau}^2\alpha\rho}{\hat{\tau}p^*(1-\overline{\beta})} \cdot \frac{\lambda}{\sin(\pi-\overline{\theta})}$$

Substituting (12), the condition becomes

$$\frac{c\overline{\tau}^2\alpha\rho}{\hat{\tau}p^*} \cdot \lambda \quad < \quad \frac{\pi(1-\overline{\beta})^2}{\sqrt{4\overline{\beta}^2+\pi^2(1-\overline{\beta})^2}}$$

Substituting λ in (15) yields the theorem. ■

The left-hand side of the (sufficient) stability condition depends on network parameters (c and τ_i) as well as RED parameters (α and ρ). The right-hand side is a property of the network node that is independent of these parameters. For stability, the left-hand side must be small. This requires small capacity c and delays τ_i and large N, confirming the simulation results of the last section. To understand this, note that $c\hat{\tau}$ is the equilibrium window size of all sources. Assuming $w_1^* = c\hat{\tau} \gg 2$ so that $p = 2/w_1^{*2}$, then the stability condition can be re-written as

$$\rho\,\frac{w_1^{*3}N}{4}\left(\frac{w_1^*}{2}+1+\frac{N}{w_1^*\alpha}\right) \quad < \quad \frac{\pi(1-\overline{\beta})^2}{\sqrt{4\overline{\beta}^2+\pi^2(1-\overline{\beta})^2}}$$

This suggests that the system becomes unstable (oscillatory) when window size w_1^* becomes large, agreeing with our empirical experience that TCP behaves poorly at large window size. Roughly, when c doubles, the equilibrium rate doubles, and hence window is halved with twice the magnitude at twice the frequency, resulting in a quadratic increase in control gain and pushing the system into instability.

The dependence of the stability condition on c, τ, and N is most clearly exhibited in the case of identical sources, with $\tau = \tau_i = \overline{\tau} = \underline{\tau} = N\hat{\tau}$.

Corollary 6 *Suppose $p = 2/w_1^{*2}$. Then the stability condition in Theorem 2 becomes*

$$\rho\,\frac{c^3\tau^3}{4N^2}\left(\frac{c\tau}{2N}+1+\frac{1}{\alpha c\tau}\right) \quad < \quad \frac{\pi(1-\overline{\beta})^2}{\sqrt{4\overline{\beta}^2+\pi^2(1-\overline{\beta})^2}}$$

The stability condition also suggests that a smaller ρ and a larger α enhance stability. A smaller ρ implies a larger equilibrium queue length [12]. A larger α incorporates the current queue length into the marking probability more quickly. If queue averaging is completely removed and the marking probabilty is proportional to instantaneous queue, $p(t) = \rho b_l(t)$, then Lemma 5 is modified to

$$A_2 \quad \subseteq \quad \frac{\overline{\tau}\rho}{\hat{\tau}p^*(1-\overline{\beta})} \cdot \left\{\eta\; e^{-j\overline{\theta}} \;:\; \mathrm{Im}\{\eta\} \geq -\lambda\right\}$$

where

$$\lambda \;:=\; \frac{1+p^*w_1^*}{(p^*w_1^*)^2}$$

and the stability condition becomes

$$\frac{\overline{\tau}\rho}{\hat{\tau}p^*}\cdot\frac{1+p^*w_1^*}{(p^*w_1^*)^2} \;<\; \frac{\pi(1-\overline{\beta})^2}{\sqrt{4\overline{\beta}^2+\pi^2(1-\overline{\beta})^2}}$$

In the case of identical sources (assuming $w_1^* \gg 2$), it becomes

$$\rho\cdot\frac{c^3\tau^3}{N^3}\left(\frac{c\tau+N}{2}\right) \;<\; \frac{\pi(1-\overline{\beta})^2}{\sqrt{4\overline{\beta}^2+\pi^2(1-\overline{\beta})^2}}$$

5 RED parameter setting

It is suggested in [5] that the RED parameter `max_p` be dynamically adjusted: reduce `max_p` as N decreases and raise it otherwise. Raising `max_p`, or reducing `max_th - min_th`, is equivalent to increasing ρ (= `max_p/(max_th-min_th)`) in the direction consistent with the stability condition in Theorem 2. Theorem 2 sets an upper bound on ρ, given N, c, τ (and α), and hence a lower bound on equilibrium queue length, to ensure stability. Adapting RED parameters *cannot* prevent the inevitable choice between stability and performance: either ρ is set small to stabilize the queue, around a large value, or, alternatively, it is set large to reduce the queue, at the risk of violent oscillation. What adaptation can hope to achieve is to dynamically find a good compromise when network condition changes.

The same stability analysis can also be applied to other AQMs, such as Virtual Queue [7, 9, 10] and REM/PI [2, 8], and clarifies the role of AQM. The stability proof relies on bounding a set of the form

$$K\cdot\mathrm{co}\{h(v,\theta)\}$$

to the right of $(-1,0)$. The gain K and the trajectory h depend on TCP as well as AQM. For instance, for the case of a single link with capacity c shared by N identical sources with delay τ, TCP and network delay contribute a factor

$$h_{tcp} \;=\; \frac{e^{-jv}}{jv+p^*w_1^*}$$

to the trajectory h and a factor

$$K_{tcp} \;=\; \frac{c^2\tau^2}{2N} \tag{16}$$

to the gain K, assuming equilibrium window is large so that $p^* = 2/w_i^2 = 2N/c\tau$. AQM compensates for the high gain introduced by TCP by shaping h and reducing K. With RED, for instance,

$$\begin{aligned} h(v,\theta) &= \frac{1}{jv + \alpha c\tau} \frac{e^{-j\theta}}{v} \cdot h_{tcp} \\ K &= \frac{c\tau\alpha\rho}{1-\beta} \cdot K_{tcp} \end{aligned}$$

The first term in h is due to RED averaging, the second term is due to queue dynamics that also bounds $\theta \leq \overline{\theta_0}$. Hence both the queue and RED add phase lag to h. More importantly, RED adds another $c\tau$ to the gain K, necessitating a small $\alpha\rho$ for stability and leading to sluggish response and large equilibrium queue. The factor $\tau/(1-\beta)$ in K comes from the queue.

The high gain K_{tcp} in (16) is mainly responsible for instability at high delay, high capacity or low load. It makes it difficult for any AQM algorithm to stabilize the current TCP.

6 A scalable control

Delay can be large in the current Internet (according to [1], 85% of the round trip time measurements range in 15–500 ms), a fact that is to some degree inevitable because of geographical distance. As network capacity scales up, the current TCP protocol will be made to operate with high window sizes; the results in the previous sections suggest that it may be ill-suited for such an environment.

It also seems difficult to design effective AQM to compensate for the high gain introduced by the current TCP. However, as we argue in this section, the problem of TCP/AQM design is not hopeless: indeed, there is enough structure for the design of simple algorithms that can maintain both linear stability and good performance. We demonstrate this by presenting an algorithm, developed in [15], that can be implemented in a decentralized way by sources and links, and that is scalable: it maintains linear stability for *arbitrary* delay, capacity, load and routing. Moreover, it achieves high network utilization in equilibrium with small queues. See [17, 16] for extensions to achieve arbitrary fairness, in addition to stability and performance, and for implementation strategies and simulation results.

The congestion control algorithm of [15] consists of a static source algorithm and a first-order dynamic link algorithm. The key idea is to compensate for delay at sources by scaling down the gain on rates by their individual round trip times, and to compensate for loop gain introduced by capacity and routing by scaling down the control gain at links by their capacities and scaling it up at sources by their current rates. In other words, a source reacts more slowly if its round trip delay is large or if its rate is small; a link updates its congestion measure (called 'price') more slowly if it has a larger capacity. Note that network delay is the *only* open-loop parameter not under our control, and it *should* set the time-scale of the system response.

Consider the network model described in Section 3.1. Let $p_l(t)$ be the price at link l at time t and c_l be a *virtual* capacity that is strictly less than real link capacity. Each link l adjusts its price

using the aggregate input rate $y_l(t) = \sum_s R_{ls} x_s(t)$:

$$\dot{p}_l(t) \quad = \quad \begin{cases} \frac{y_l - c_l}{c_l} & \text{if } p_l > 0; \\ \max\{0, \frac{y_l - c_l}{c_l}\} & \text{if } p_l(t) = 0 \end{cases} \tag{17}$$

Therefore prices integrate excess capacity in a normalized way, and are saturated to be always non-negative. At equilibrium, bottlenecks with nonzero price will have $y_l^* = c_l$, giving high utilization. Non-bottlenecks with $y_l^* < c_l$ will have zero price. Since c_l is less than real capacity, queue is negligible in equilibrium. If c_l were the real capacity, $p_l(t)$ would be the real queueing delay, a congestion signal used in TCP Vegas [13].

Let $x_i(t)$ be the rate of source i at time t, τ_i its round trip time (assumed constant), and M_i the number of congested links in its path (or an upper bound). Given aggregate price $q_i(t) = \sum_l R_{li} p_l(t)$, source i sets its rate to be exponential in $q_i(t)$:

$$x_i(t) \quad = \quad x_{\max,i}\, e^{-\frac{\alpha_i q_i(t)}{M_i \tau_i}} \tag{18}$$

Here $x_{\max,i}$ is a maximum rate parameter, and $\alpha \in (0, 1)$. The utility function corresponding to the source control is

$$U_i(x) = \frac{M_i \tau_i}{\alpha_i} x \left[1 - \log\left(\frac{x}{x_{\max,i}}\right)\right], \quad \text{for } x \le x_{\max,i};$$

Suppose the routing matrix R has full row rank. Then there is a unique equilibrium rate and price vector (x^*, p^*). The linearized system around the equilibrium is described by:

$$\delta\dot{p}_l(t) \quad = \quad \frac{\delta y_l(t)}{c_l}, \qquad \text{for all } l \tag{19}$$

$$\delta x_i(t) \quad = \quad -\frac{\alpha_i x_i^*}{M_i \tau_i} \delta q_i(t), \qquad \text{for all } s \tag{20}$$

where the source rates $\delta x(t)$ and link prices $\delta p(t)$ are interconnected by the delayed routing matrices defined in (9–10).

The following theorem, proved in [15], guarantees the stability of the algorithm when the network scales up arbitrarily in delay, capacity and load.

Theorem 7 ([15]) *Suppose all links included in R are bottlenecks, i.e., $c = Rx^*$ in equilibrium, and R has full row rank. Then the closed-loop system described by (19–20) and (9–10) is linearly stable for* arbitrary *delays τ_i and link capacities c_l.*

7 Conclusion

We have presented simulation results to demonstrate that it is protocol stability more than other factors that determines the dynamics of TCP/RED. We have developed a multi-link multi-source model that can be used to study the stability of general TCP/AQM. We have presented a sufficient stability condition for the case of a single link with heterogeneous sources, and illustrated the form of TCP/RED's stability region. It implies that TCP/RED becomes unstable when the network scales up in delay or capacity. Our analysis indicates the role, and the difficulty, of RED in stabilizing TCP. We have demonstrated that it is possible to maintain both local stability and good performance, such as high utilization and low queue, for arbitrary delay, capacity, load and routing.

We close by commenting on the importance of protocol stability. There is currently no theory to understand the behavior of a distributed nonlinear feedback system with delay when the system loses stability. It is therefore undesirable to operate in unstable regime, and unnecessary if stability can be maintained without sacrificing performance. In fact, instability can cause three problems. First, it increases jitters in source rate and delay and can be detrimental to some applications. Second, it subjects short-duration connections, that are typically delay and loss sensitive, to unnecessary delay and loss. Finally, it can lead to under-utilization of network links if queues jump between empty and full.

8 Appendix: Proofs

8.1 Proof of Lemma 3

Let the denominator of the last term in (13) at $s = j\omega$ be:

$$\begin{aligned}\lambda(j\omega) &:= j\omega + \sum_n \frac{x_n^*}{c}\frac{e^{-j\beta_n\tau_n\omega}}{\tau_n} \\ &= j\omega\left(1+\overline{\beta}\left(\sum_n \frac{\beta_i}{\overline{\beta}}\frac{x_n^*}{c}\frac{e^{-j\beta_n\tau_n\omega}}{j\beta_n\tau_n\omega} + \left(1-\sum_n \frac{\beta_i}{\overline{\beta}}\frac{x_n^*}{c}\right)\cdot 0\right)\right)\end{aligned}$$

i.e., $\lambda(j\omega)$ is a convex sum of the N points $e^{-j\beta_n\tau_n\omega}/j\beta_n\tau_n\omega$ and the origin. Since the origin is also on the line e^{-jv}/jv at $v=\infty$, we have

$$\frac{\lambda(j\omega)}{\omega} \in \left\{ j(1+\overline{\beta}\zeta) \;:\; \zeta \in \mathrm{co}\left\{ \frac{e^{-jv}}{jv} \;:\; v \geq 0 \right\} \right\}$$

where co$A$ is the convex hull of set A. For $v \geq 0$, let

$$\zeta(v) = \frac{e^{-jv}}{jv} = -\frac{\sin v}{v} - j\frac{\cos v}{v} =: a(v) + jb(v) \tag{21}$$

The real part of ζ is bounded by $-1 \le a(v) < 1/\pi$; the imaginary part of ζ is bounded by $b(v) < 2/\pi$. Hence

$$\mathrm{co}\left\{ \frac{e^{-jv}}{jv} \ : \ v \ge 0 \right\} \ \subseteq \ \{a + jb \ : \ -1 \le a \le 1/\pi, \ b \le 2/\pi\}$$

and

$$\left(\frac{\lambda(j\omega)}{\omega}\right)^{-1} \ \in \ \left\{ \frac{1}{-\overline{\beta}b + j(1+\overline{\beta}a)} \ : \ -1 \le a \le 1/\pi, \ b \le 2/\pi \right\} \tag{22}$$

Since $1 - \overline{\beta} > 0$, we can bound its magnitude and phase:

$$\left| \left(\tfrac{\lambda(j\omega)}{\omega}\right)^{-1} \right| \ \le \ \frac{1}{1-\overline{\beta}} \tag{23}$$

$$0 \ \le \ \angle \left(\tfrac{\lambda(j\omega)}{\omega}\right)^{-1} \le \ \overline{\theta} \tag{24}$$

where $\overline{\theta}$ is defined in (12).

From (13), for all i,

$$z_i(j\omega) \ = \ \frac{\tau_i^2 e^{-j\tau_i\omega}}{\tau_i\omega(j\tau_i\omega + \alpha c\tau_i)(j\tau_i\omega + p^* w_i^*)} \cdot \left(\frac{\lambda(j\omega)}{\omega}\right)^{-1} \tag{25}$$

From (14), we have

$$L(j\omega) \ \in \ \frac{c\alpha\rho}{\hat{\tau}p^*} \cdot \mathrm{co}\{z_i(j\omega), i = 1, \ldots, N\}$$

Since $z_i(j\omega)$ is the origin at $\omega = \infty$ and that $w_i^* = w_1^*$ for all i, it can be shown that the above convex set is contained in the following larger set, obtained by replacing τ_i by $\overline{\tau} := \max_i \tau_i$ in the numerator and by $\underline{\tau} := \min_i \tau_i$ in the denominator in (25) and using (23–24):

$$L(j\omega) \ \in \ \frac{c\overline{\tau}^2\alpha\rho}{\hat{\tau}p^*(1-\overline{\beta})} \cdot \mathrm{co}\left\{ r(\omega)e^{-j\phi(\omega)} \cdot e^{-j\theta} \ : \ 0 \le \theta \le \overline{\theta}, \ \omega \ge 0 \right\}$$

where $r(\omega)e^{-j\phi(\omega)}$ is defined in the lemma. ■

8.2 Proof of Lemma 4

Fix any point $\eta = \sum_i a_i\eta_i$ in A_1, where $a_i \ge 0$, $\sum_i a_i = 1$, and where $\eta_i := r(\omega_i)e^{-j\phi(\omega_i)} \cdot e^{-j\theta_i}$ are points on the Nyquist trajectory $N(\theta_i)$ defined by θ_i. We will show that η is a convex sum of points on the Nyquist trajectory $N(\overline{\theta})$ defined by $\overline{\theta}$ and hence is in the right hand side.

For each θ_i, define $\hat{\omega}_i$ by $\phi(\hat{\omega}_i) + \overline{\theta} = \phi(\omega_i) + \theta_i$. Then $0 \le \hat{\omega}_i \le \omega_i$ since $\phi(\omega)$ is increasing in ω. Since $r(\omega)$ is decreasing in ω, the point η_i lies on the line segment from the origin to $\hat{\eta}_i := r(\hat{\omega}_i)e^{-j\phi(\hat{\omega}_i)} \cdot e^{-j\overline{\theta}}$. Both the origin and $\hat{\eta}$ are on the Nyquist trajectory $N(\overline{\theta})$ and hence $\eta_i = b_i\hat{\eta}_i$ for some $0 \le b_i \le 1$. Hence

$$\eta \;=\; \sum_i a_i b_i \hat{\eta}_i + (1 - \sum_i a_i b_i) \cdot 0$$

i.e., η is a convex sum of points on $N(\overline{\theta})$, proving the lemma. ■

8.3 Proof of Lemma 5

First note that if

$$\eta(j\omega) \;=\; \frac{e^{-j\omega}}{\omega(j\omega + a_1)(j\omega + a_2)}$$

then for all ω

$$\mathrm{Im}\{\eta(j\omega)\} \;\ge\; -\frac{1}{a_1 a_2}\left(1 + \frac{1}{a_1} + \frac{1}{a_2}\right)$$

with equality at $\omega = 0$. To see this, we have

$$\begin{aligned}
\mathrm{Im}\{\eta(j\omega)\} &\ge -\frac{(a_1 + a_2)\omega\cos\omega + (a_1 a_2 - \omega^2)\sin\omega}{\omega(\omega^2 + a_1^2)(\omega^2 + a_2^2)} \\
&= -\left(\frac{(a_1 + a_2)\cos\omega}{(\omega^2 + a_1^2)(\omega^2 + a_2^2)} + \frac{(a_1 a_2 - \omega^2)}{(\omega^2 + a_1^2)(\omega^2 + a_2^2)} \cdot \frac{\sin\omega}{\omega}\right) \\
&\ge -\frac{1}{a_1 a_2}\left(1 + \frac{1}{a_1} + \frac{1}{a_2}\right)
\end{aligned}$$

with equality at $\omega = 0$. Then, the assertion follows from the definition of A_2 in Lemma 4 ■

References

[1] Mark Allman. A web server's view of the transport layer. *ACM Computer Communication Review*, 30(5), October 2000.

[2] Sanjeewa Athuraliya, Victor H. Li, Steven H. Low, and Qinghe Yin. REM: active queue management. *IEEE Network*, 15(3):48–53, May/June 2001. Extended version in *Proceedings of ITC17*, Salvador, Brazil, September 2001. `http://netlab.caltech.edu`.

[3] Lawrence S. Brakmo and Larry L. Peterson. TCP Vegas: end-to-end congestion avoidance on a global Internet. *IEEE Journal on Selected Areas in Communications*, 13(8):1465–80, October 1995. `http://cs.princeton.edu/nsg/papers/jsac-vegas.ps`.

[4] M. Christiansen, K. Jeffay, D. Ott, and F. D. Smith. Tuning RED for web traffic. In *Proceedings of ACM Sigcomm*, 2000.

[5] W. Feng, D. Kandlur, D. Saha, and K. Shin. A self–configuring RED gateway. In *Proceedings of INFOCOM'99*, March 1999. `http://www.eecs.umich.edu/~wuchang/work/infocom99.ps.Z`.

[6] Victor Firoiu and Marty Borden. A study of active queue management for congestion control. In *Proceedings of IEEE Infocom*, March 2000.

[7] R. J. Gibbens and F. P. Kelly. Resource pricing and the evolution of congestion control. *Automatica*, 35:1969–1985, 1999.

[8] C.V. Hollot, V. Misra, D. Towsley, and W.B. Gong. Analysis and design of controllers for AQM routers supporting TCP flows. *IEEE Transactions on Automatic Control*, 47(6), 2002.

[9] Srisankar Kunniyur and R. Srikant. End–to–end congestion control schemes: utility functions, random losses and ECN marks. In *Proceedings of IEEE Infocom*, March 2000. `http://www.ieee-infocom.org/2000/papers/401.ps`.

[10] Srisankar Kunniyur and R. Srikant. A time–scale decomposition approach to adaptive ECN marking. In *Proceedings of IEEE Infocom*, April 2001. `http://comm.csl.uiuc.edu:80/~srikant/pub.html`.

[11] S. H. Low, F. Paganini, J. Wang, S. A. Adlakha, and J. C. Doyle. Dynamics of TCP/RED and a scalable control. In *Proc. of IEEE Infocom*, June 2002. `http://netlab.caltech.edu`.

[12] Steven H. Low. A duality model of TCP and queue management algorithms. *IEEE/ACM Trans. on Networking, to appear*, October 2003. `http://netlab.caltech.edu`.

[13] Steven H. Low, Larry Peterson, and Limin Wang. Understanding Vegas: a duality model. *J. of ACM*, 49(2):207–235, March 2002. `http://netlab.caltech.edu`.

[14] Martin May, Thomas Bonald, and Jean-Chrysostome Bolot. Analytic evaluation of RED performance. In *Proceedings of IEEE Infocom*, March 2000.

[15] Fernando Paganini, John C. Doyle, and Steven H. Low. Scalable laws for stable network congestion control. In *Proceedings of Conference on Decision and Control*, December 2001. `http://www.ee.ucla.edu/~paganini`.

[16] Fernando Paganini, Zhikui Wang, John C. Doyle, and Steven H. Low. Congestion control for high performance, stability and fairness in general networks. submitted for publication, March 2003.

[17] Fernando Paganini, Zhikui Wang, Steven H. Low, and John C. Doyle. A new TCP/AQM for stability and performance in fast networks. In *Proc. of IEEE Infocom*, April 2003. `http://www.ee.ucla.edu/~paganini`.

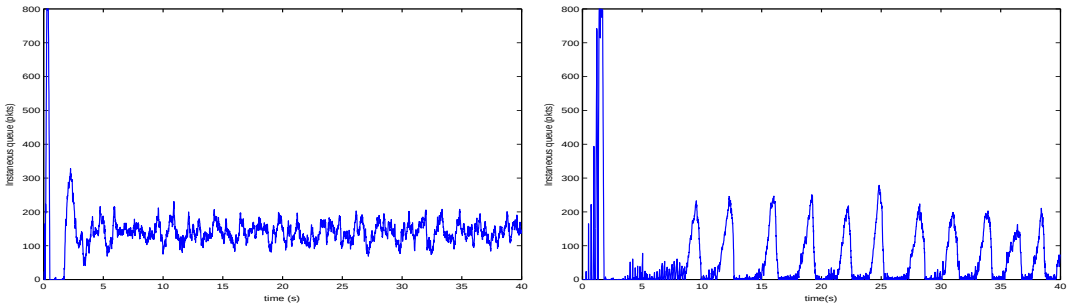

(a) Queue (delay = 40ms, 10% noise)

(b) Queue (delay = 200ms, 10% noise)

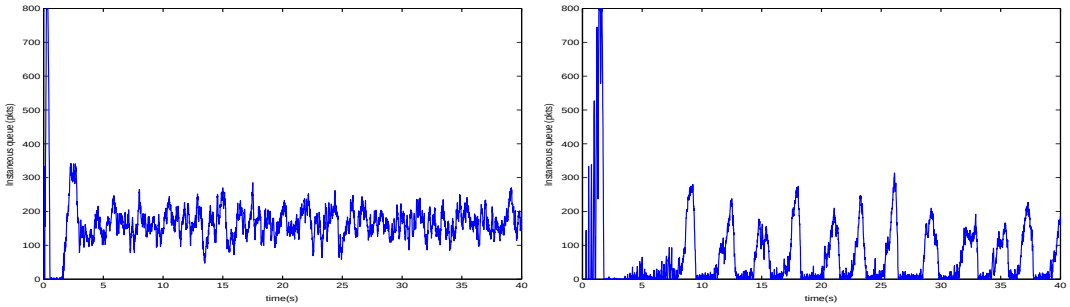

(c) Queue (delay = 40ms, 30% noise)

(d) Queue (delay = 200ms, 30% noise)

Figure 2: Queue traces with noise traffic. Simulation parameters: 50 sources, capacity = 9 pkts/ms, RED = (0.1, 50, 550, 10^{-4}), marking with 'byte' mode; two-way traffic.

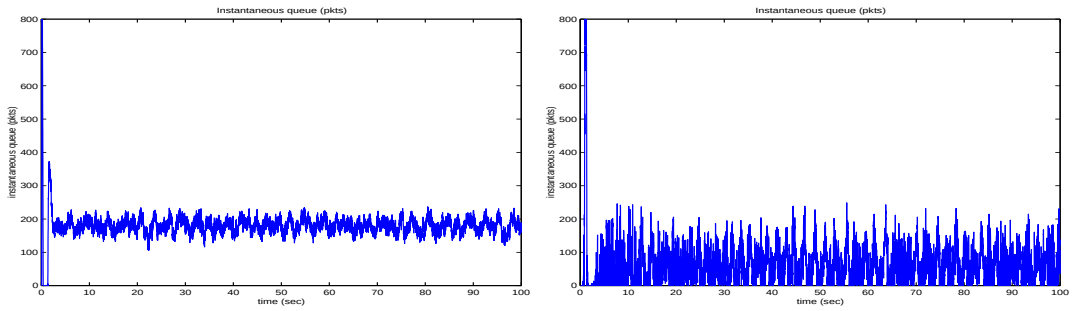

(a) Queue (delays from 12ms to 19ms)

(b) Queue (delays from 160ms to 254ms)

Figure 3: Queue traces with heterogeneous delays. Simulation parameters: 50 sources, capacity = 9 pkts/ms, RED = (0.1, 50, 550, 10^{-4}), marking with 'byte' mode; one-way traffic.

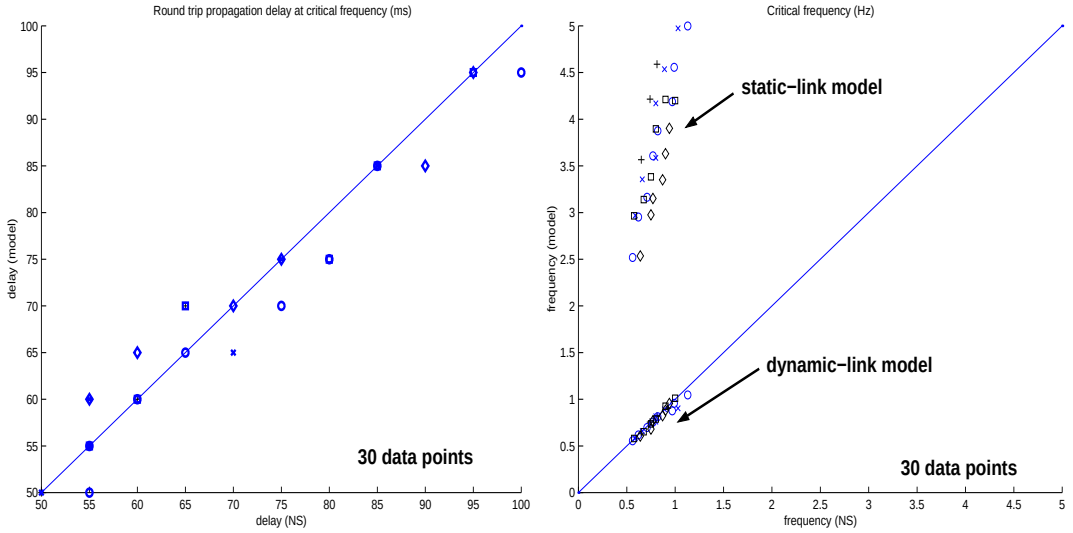

(a) Critical delay (ms)

(b) Critical frequency (Hz)

Figure 4: Validation.

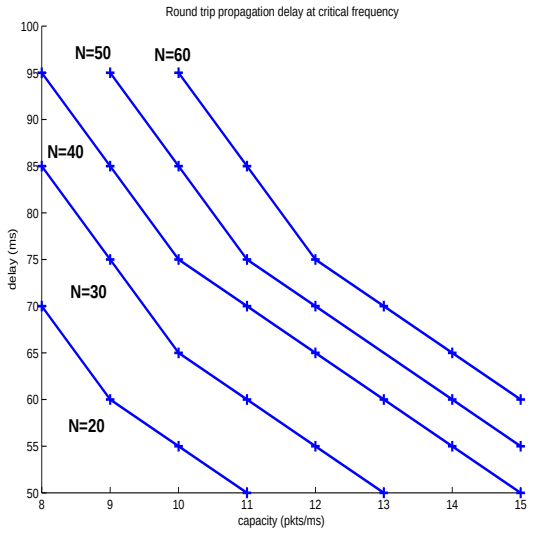

Figure 5: Stability region: for each N, the region above the curve is unstable and that below is stable.

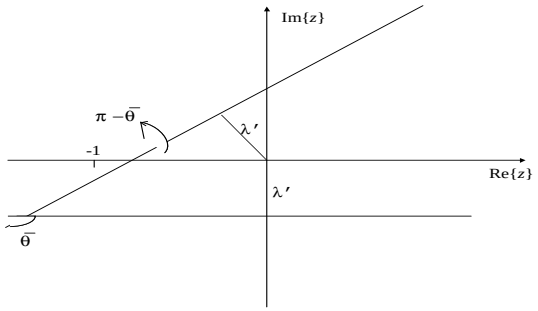

Figure 6: Proof of Theorem 2 with $\lambda' = \lambda \cdot c\overline{\tau}^2\alpha\rho/\hat{\tau}p^*(1-\overline{\beta})$.